RESEARCH ARTICLE

Anastomotic stoma coated with chitosan film as a betamethasone dipropionate carrier for peripheral nerve regeneration

Ping Yao[1,#], Peng Li[2,#], Jun-jian Jiang[3,*], Hong-ye Li[4,*]
1 Department of Hand Surgery, Hangzhou Plastic Surgery Hospital, Hangzhou, Zhejiang Province, China
2 Department of Anesthesia, Affiliated Puai Hospital of Huazhong University of Science and Technology, Wuhan, Hubei Province, China
3 Department of Hand Surgery, Huashan Hospital, Fudan University, Shanghai, China
4 Department of Hand Surgery, Sir Run Run Shaw Hospital, School of Medicine, Zhejiang University, Hangzhou, Zhejiang Province, China

Graphical Abstract

Chitosan film as a betamethasone dipropionate carrier promotes tibial nerve regeneration

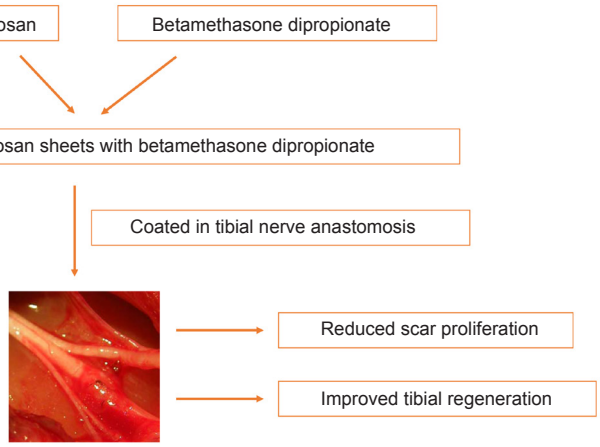

***Correspondence to:**
Jun-jian Jiang, M.D., Ph.D. or Hong-ye Li, jjjdoctor@126.com or swrhxy@yeah.net.

#These authors contributed equally to this paper.

orcid:
0000-0001-6087-1308 (Jun-jian Jiang)
0000-0001-9823-1277 (Hong-ye Li)

doi: *10.4103/1673-5374.226401*

Accepted: *2017-11-05*

Abstract

Scar hyperplasia at the suture site is an important reason for hindering the repair effect of peripheral nerve injury anastomosis. To address this issue, two repair methods are often used. Biological agents are used to block nerve sutures and the surrounding tissue to achieve physical anti-adhesion effects. Another agent is glucocorticosteroid, which can prevent scar growth by inhibiting inflammation. However, the overall effect of promoting regeneration of the injured nerve is not satisfactory. In this regard, we envision that these two methods can be combined and lead to shared understanding for achieving improved nerve repair. In this study, the right tibial nerve was transected 1 cm above the knee to establish a rat tibial nerve injury model. The incision was directly sutured after nerve transection. The anastomotic stoma was coated with 0.5 × 0.5 cm^2 chitosan sheets with betamethasone dipropionate. At 12 weeks after injury, compared with the control and poly (D, L-lactic acid) groups, chitosan-betamethasone dipropionate film slowly degraded with the shape of the membrane still intact. Further, scar hyperplasia and the degree of adhesion at anastomotic stoma were obviously reduced, while the regenerated nerve fiber structure was complete and arranged in a good order in model rats. Electrophysiological study showed enhanced compound muscle action potential. Our results confirm that chitosan-betamethasone dipropionate film can effectively prevent local scar hyperplasia after tibial nerve repair and promote nerve regeneration.

Key Words: *nerve regeneration; chitosan; betamethasone dipropionate; scar; nerve injury; repair; function restoration; film; drug release; carrier; neural regeneration*

Introduction

Peripheral nerve lesions are common and severe injuries that impact 2.8% of traumatic patients annually, and result in lifetime disability if unattended (Belkas et al., 2004). Nowadays, various methods are used to guide regenerating nerve fibers into the correct distal endoneurial tubes during surgical repair. The most-used strategies developed for nerve repair include end-to-end suturing of nerve stumps and bridging by autografts (Isaacs et al., 2008). However, a major problem for nerve repair is the formation of fibroblastic scars at the site of neuroanastomosis (Ngeow, 2010). Even with well repaired nerve, half of the regenerating axons may grow into scar tissue, which leads to local neuroma and impedes axonal regeneration to the target (Sedy, 2010). Consequently, regenerating nerve function is generally far from satisfactory.

Thus, production of fibroblastic scars during nerve anastomosis impedes the regeneration of repaired nerves.

Nowadays, two kinds of treatments are used. Biological agents that separate the site of nerve anastomosis from the surrounding tissue to achieve the effect of physical protection, namely sodium hyaluronate and poly (D, L-lactic acid) (PDLLA) (Ganguly et al., 2004; Takezawa et al., 2007), while another type of agent is glucocorticosteroid, which prevents scar growth by inhibiting inflammation (Grauer et al., 2001). Combining these strategies with biological or synthetic materials for repairing damaged peripheral nerves is of utmost interest. Among them, synthetic tubes seeded with Schwann cells to facilitate axonal regeneration are the most widely used (Ghaznavi et al., 2011; Joseph et al., 2011). Unfortunately, Schwann cells secrete major histocompatibility complex class I, which occupies the most gene-dense region of the mammalian genome and plays a key role in immune system recognition and transplantation. Consequently, there has been controversy concerning the use of allogeneic Schwann cells for nerve repair owing to their specific immunogenicity. Recently, synthetic tubes seeded with aligned neural stem cells were found to promote axonal regeneration of a nerve defect in a rat model (Hsu et al., 2009). However, biological agents are barely usable because of rapid degradation and absorption in the body, which means there is no long-term practical application of transplanted biological agents (Eillitz-Markus et al., 2012).

Chitosan is an alkaline-deacetylated chitin derived from the exoskeleton of insects and shell of crustaceans. It is a biodegradable polysaccharide comprised of glucosamine and N-acetylglucosamine (Jayakumar et al., 2007; Barahuie et al., 2017; Liang et al., 2017; Qiu et al., 2017; Vaden-Braber et al., 2017; Zheng et al., 2017). Since chitosan can accelerate wound healing, it has been widely used in various biomedical treatments. Chitosan is biocompatible and biodegradable (Mi et al., 2001; Okamoto et al., 2002), and has recently become the focal point of many studies (Arkoun et al., 2017; Praphakar et al., 2017).

Betamethasone dipropionate is a glucocorticoid that is usually for external use or injection. Betamethasone dipropionate plays an important role in Th lineage development (for instance favoring generation of Th2 cells), downregulation of fasL expression, and inhibition of activation-induced T cell apoptosis (Kim et al., 2017; Paul et al., 2017). Glucocorticoids are also potent inducers of apoptosis, which can cause the death of $CD4^+CD8^+$ thymocytes at concentrations achieved during the stress response (Lovato et al., 2016; Queille-Roussel et al., 2016).

Many drug delivery systems derived from chitosan have been developed (Janes et al., 2001; Mitra et al., 2001; Mi et al., 2002; Abarrategi et al., 2008), which can be released gradually to improve treatment effect. To develop optimal drug activity, the quality and shape of the carrier have a pivotal effect. In our study, a flexible flat chitosan sheet was produced by a simple technique, and we subsequently observed chitosan biodegradation and drug (betamethasone dipropionate) release from the chitosan sheet. This system will enable us to investigate the feasibility of chitosan as a drug delivery system for repairing peripheral nerve lesions.

Materials and Methods

Animals

Seventy-two male Wistar rats aged 5–6 weeks and weighing 120 g were obtained from the Experimental Animal Center of Chinese Academy of Sciences (SYXK (Hu) 2013-0062). After anesthesia, the surgical area (right leg of each rat) was shaved and disinfected. The tibial never was cut 1 cm above the knee, and nerve stumps sutured immediately under a microscope (Yohn et al., 2008). Sheets (0.5 cm × 0.5 cm) were coated in nerve anastomosis. Rats were placed in individual cages and allowed free access to food and water.

The study protocol was approved by the Animal Ethics Committee of Hangzhou Plastic Surgery Hospital of China (approval number: LY12H05005). The experimental procedure followed the *United States National Institutes of Health Guide for the Care and Use of Laboratory Animal* (NIH Publication No. 85-23, revised 1986).

All rats were randomly divided into three groups before treatment: control group (n = 24; treatment by direct suture after nerve transection); PDLLA group (n = 24; PDLLA was coated in nerve anastomosis); chitosan-betamethasone dipropionate film group (n = 24; chitosan sheets with betamethasone dipropionate were coated in nerve anastomosis).

Chitosan formation

To form chitosan, heterogeneous deacetylation of chitin (Sigma, St. Louis, MO, USA) was performed using 50% (w/w) NaOH heated for 60 minutes at 136°C. Chitosan was characterized using the American Society for Testing and Materials (ASTM) F2103-01 standard as follows: acetylation degree 16.0 ± 0.7% (^{1}H NMR measurements), moisture content 5.3 ± 0.5%, dust burden 0.39 (0.10%; and equal viscosity molecular weight 56,100 g/mol [solvent system 0.3 M AcOH/0.2 M AcONa]). The standard for the Mark-Houwink equation "K" and "a" constant were 1.28×10^{-2} and 0.85, respectively. Other constants were used to gain molecular weight (Heux et al., 2000). Viscosity was measured using an Ubbelohde viscometer (Schott Geräte TYP 52520/II, Bremen, Germany).

Chitosan sheet formation and betamethasone dipropionate incorporation

Depolymerization was implemented by agitating chitosan solution with 15 mL of 31.36 mM KNO_2 for 2 hours at 35°C. Acetone was added to depolymerized chitosan to stop the reaction. A sterile 0.22 μm filter was used to filter 1% (w/v) chitosan solution (50 mM acetic acid), which was possible because of the water and ash content. Next, 200 μL aliquots were layered over 1 cm^2 surface dishes. The solvent was allowed to evaporate from open plates in a sterile laminar flow hood overnight at room temperature. Sheets were incubated with buffer phosphate (0.25 M, pH 7.0), and extensively washed with phosphate buffered saline (PBS). Betamethasone dipropionate 1 mL (1 g/mL) was added to the initial chitosan solution when necessary.

Swelling studies

After formation of sheets, dry sheets were weighed and im-

mersed in PBS at 37°C under continuous agitation. Surface PBS was removed using dry tissue and the sheets weighed again. Swelling percentage was measured as follows: S% = (wet sample weight – dry sample weight)/dry sample weight × 100.

Betamethasone dipropionate diffusion assay

Betamethasone dipropionate concentration was calculated by high-performance liquid chromatography (HPLC). An HPLC column with a fluorescence detector (F1050; Hitachi, Tokyo, Japan) was used for analysis. The stationary phase was a normal phase column (Mightysil Si60; Kanto Kagaku, Tokyo, Japan), and the mobile phase was chloroform-isopropanol-acetic acid-water-sodium acetate buffer (100:100:14:14:1, pH 4.5) at a flow rate of 1.0 mL/min. Fluorescent signals were surveyed at 470 nm excitation and 585 nm emission. Betamethasone dipropionate was extracted by chloroform/methanol (4:1) and then centrifuged at 15,000 r/min for 15 minutes. The phase-separated chloroform/methanol layer was analyzed by HPLC. Pure betamethasone dipropionate was used as the standard. The content of betamethasone dipropionate absorbed by the chitosan sheets was 1 μg/mg dry chitosan. Fluorescence microscopy was used to confirm absorption of betamethasone dipropionate.

Sheet bioactivity assays

Sheets were treated as described above. L929 fibroblasts were purchased from Invitrogen Corp. (Carlsbad, CA, USA). Cells were cultured in RPMI-medium 1640 containing 15% fetal bovine serum, L-glutamine, and penicillin-streptomycin at 37°C in an atmosphere of 5% CO_2. The culture medium was replaced every 3 days. Next, cells were layered onto sheets at a density of 2×10^3 cells/well in 96-well tissue culture clusters (Corning Costar, New York, NY, USA). At specific time intervals, six samples from each sheet group were gently rinsed twice with sterile PBS solution to remove dead cells, and 3-(4,5-dimethylthiazol-2-yl)-2,5-diphenyltetrazolium bromide (MTT) assays performed to quantify cell viability.

Sheet stability at different pH values

Dry sheets were saturated in different pH buffer solutions from pH 3 to pH 7.4 at 37°C. Samples were taken at selected time points. Chitosan content was determined by colorimetric assay (Cibacron Brilliant Red 3B-A, TX, USA) and shown as a percentage of total chitosan amount initially present in the sheet.

In brief, 10 μL/well of lysis buffer (50 mM Tris, 0.1% Triton X-100, 2 mM $MgCl_2$) was mixed. For activity, 10 μL samples were analyzed in 96-well plates at 37°C. The substrate was p-nitrophenylphosphate in 2-amino-2-methyl-1-propanol buffer in a total volume of 100 μL. After 10 minutes, the reaction was stopped with 100 μL of 0.5 M NaOH. Finally, absorbance was calculated at 450 nm using a microplate reader (Biotek FL-600; Christiansburg, VA, USA).

***In vitro* enzymatic degradation**

In vitro degradation of chitosan films (1 cm^2 performed on 48-well plates) was performed with 500 μg/mL lysozyme (hen egg white; Sigma) in 1 mL PBS (pH 7.4) at 37°C. At selected time points, the enzyme solution was replaced every other day, and then 1 mL of acetic acid mixed to dissolve the remaining sheet. Sequentially, enzymatic degradation of chitosan sheets was performed in 1 mL of 0.2 M acetate buffer solution (pH 5.4) by the same procedure. An automated microviscometer (Anton Paar, Graz, Austria) was used to measure dynamic viscosity of the solution.

Evaluation of betamethasone dipropionate retained in sheets after enzymatic hydrolysis

In vitro enzymatic degradation of chitosan sheets was performed as described above. The remaining film was dissolved in acetic acid at exposition days 1, 4, 7, 11, and 14. Betamethasone dipropionate was calculated by colorimetric assay as previously described (see Sheet stability at different pH values).

Immunohistochemistry

The animals were killed by anesthesia at 12 weeks after surgery. Tissue samples of the tibias nerve were taken, and the specimens preserved in 2.5% glutaraldehyde and embedded in araldite. Serial 20 μm-thick longitudinal sections were taken through the suture site of the tibias nerve. Sections were rinsed twice with 0.01 M PBS, followed by immunohistochemical staining of nerve fibers using mouse anti-neurofilament (NF) monoclonal antibody (dilution 1:200; Abcam, Cambridge, MA, USA) to evaluate axonal regeneration at the suture site. Afterwards, sections were treated at 4°C overnight and washed three times with cold PBS. Then, fluorescent secondary antibody fluorescein isothiocyanate (goat anti-mouse IgG-TITC, dilution 1:100; Santa Cruz Biotechnology, Santa Cruz, CA, USA) was added for 2 hours. Sections were examined with a BX53 fluorescence microscope at 100× magnification.

Electrophysiological evaluation

At 8 and 12 weeks after surgery, electrophysiological recordings were performed using Medelec Synergy (Viasys Healthcare Inc., Conshohocken, PA, USA) in a quiet room at 22–23°C. All recordings were performed with a subcutaneous needle electrode. Nerve conduction tests of nerve fibers were performed, including motor nerve conduction velocity (MNCV) and compound muscle action potential (CMAP). For CMAP, the active electrode was inserted to the middle of gastrocnemius, the reference electrode on the muscle tendon in the silent region of the distal extremity, and a ground electrode externally on the animal's thorax. The tibial nerve was stimulated at the tibial notch 1.5 cm proximal to the injured region by adjusting the distance between the cathode and anode to 1 cm. Supramaximal pulses (usually 0.05 ms in duration) were delivered. To reduce artifacts, stimulus

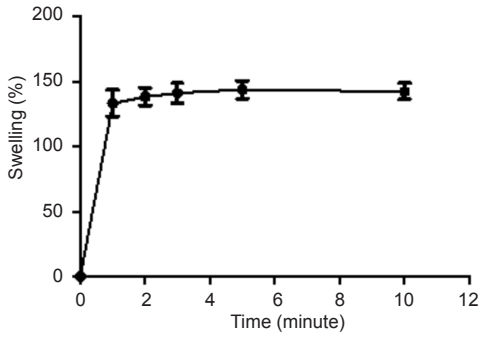

Figure 1 Swelling rate of chitosan film with betamethasone dipropionate.
Dried and neutralized sheets were soaked in phosphate buffered solution at 37°C. Swelling rate was determined by gravimetric test. Data demonstrate percentage of swelling (mean ± SD, n = 24, non-linear regression fitting analysis). The experiment was performed in triplicate.

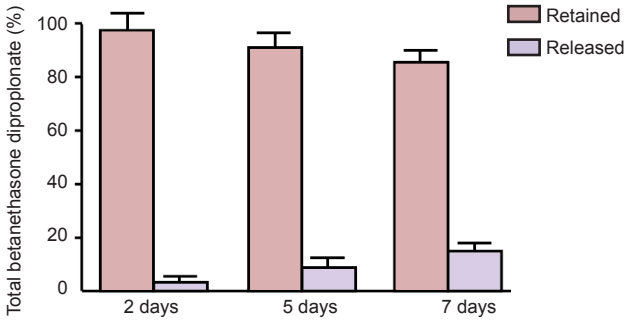

Figure 2 Drug release test in phosphate buffered saline at 37°C.
Films incorporating drug were immersed in phosphate buffered solution and aliquots collected over the time course. Afterwards, released drug content was measured. Remaining drug content was measured by dissolution of the remaining film (mean ± SD, n = 24). The experiment was performed in triplicate.

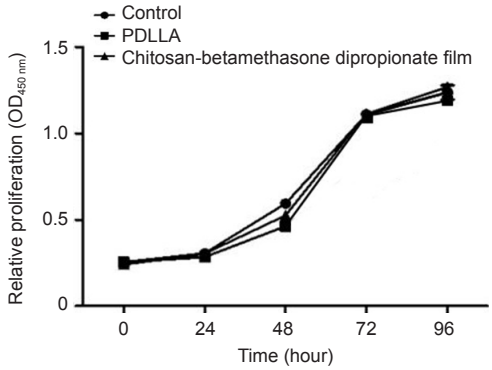

Figure 3 Sheet bioactivity assays.
In vitro 3-(4,5-dimethylthiazol-2-yl)-2,5-diphenyltetrazolium bromide assay shows that cell viability is not significant in control, PDLLA, and chitosan-betamethasone dipropionate film groups (mean ± SD, n = 6, analysis of variance followed by Bonferroni *post hoc* test). The experiment was performed in triplicate. Control group: Treatment by direct suture after nerve transection; PDLLA group: PDLLA was coated in nerve anastomosis; Chitosan-betamethasone dipropionate film group: chitosan sheets with betamethasone dipropionate were coated in nerve anastomosis. PDLLA: Poly (D, L-lactic acid).

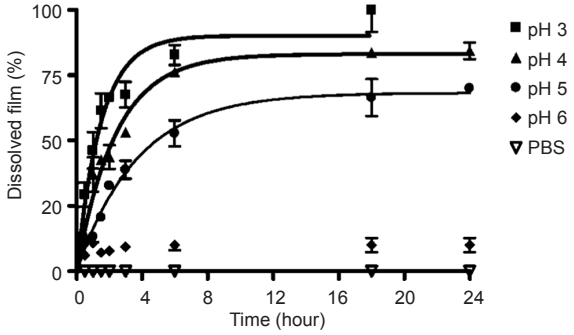

Figure 4 Sheet stability at several pH values at 37°C.
Sheets were immersed in several pH values [pH 3, pH 4, pH 5, pH 6, and phosphate buffered saline (pH 7.4)] as shown, and the amount of chitosan measured. The results are shown as percentage of total chitosan in the film, and were used in an exponential association model (mean ± SD, n = 24). The experiment was performed in triplicate. Control group: Treatment by direct suture after nerve transection; PDLLA group: PDLLA was coated in nerve anastomosis; chitosan-betamethasone dipropionate film group: chitosan sheets with betamethasone dipropionate were coated in nerve anastomosis. PDLLA: Poly (D, L-lactic acid).

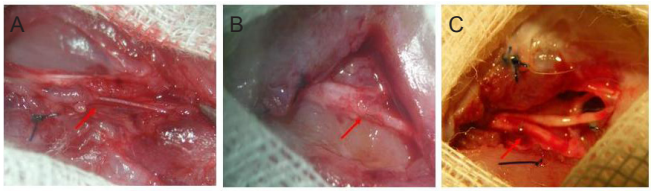

Figure 5 General examination at 12 weeks after surgery.
(A) Tibial nerves adhered to scars but with restricted movement in the control group because of markedly proliferated scars (control group). (B) Scar formation was not significant in the PDLLA group. (C) Chitosan-collagen betamethasone dipropionate film had completely degraded and scar proliferation surrounding the tibial nerve was barely seen in the chitosan-betamethasone dipropionate film group. Arrows: Adhered tibial nerves. Control group: Treatment by direct suture after nerve transection; PDLLA group: PDLLA was coated in nerve anastomosis; chitosan-betamethasone dipropionate film group: chitosan sheets with betamethasone dipropionate were coated in nerve anastomosis. PDLLA: Poly (D, L-lactic acid).

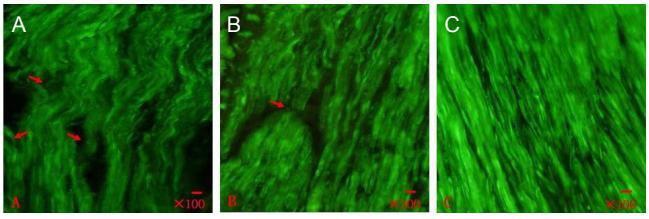

Figure 6 Immunohistochemical staining of nerve fiber (fluorescence microscope).
Immunohistochemical staining (mouse anti-neurofilament monoclonal antibody) at the suture site (longitudinal section) was performed at 12 weeks after surgery. (A) Control group: Regenerative nerve fibers were twisted and had poor alignment (arrows). (B) PDLLA group: Regenerative nerve fibers were increased and well-arranged. (C) Chitosan-betamethasone dipropionate film group: Regenerative nerve fibers were straight with more fibers than in the control group and PDLLA group. Scale bar: 1 μm. Control group: Treatment by direct suture after nerve transection; PDLLA group: PDLLA was coated in nerve anastomosis; chitosan-betamethasone dipropionate film group: chitosan sheets with betamethasone dipropionate were coated in nerve anastomosis. PDLLA: Poly (D, L-lactic acid).

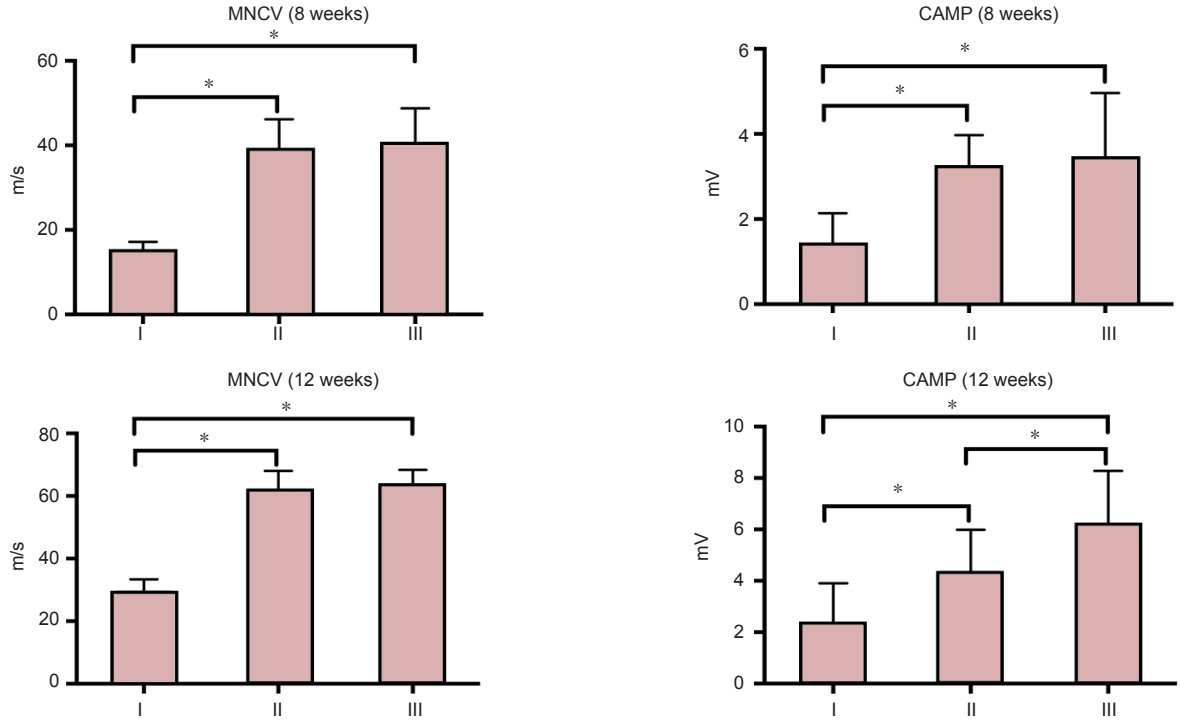

Figure 7 Electrophysiological nerve indices after repair with chitosan film and betamethasone dipropionate.
Electrophysiological study at 8 and 12 weeks after surgery. CMAP in the chitosan-betamethasone dipropionate film group was markedly higher than in the PDLLA and control groups, while CMAP was higher in the PDLLA group than the control group. Asterisks show statistically significant differences. ∗$P < 0.05$ (mean ± SD, $n = 24$, analysis of variance followed by Bonferroni *post hoc* test). I: Control group: Treatment by direct suture after nerve transection; II: PDLLA group: PDLLA was coated in nerve anastomosis; III: chitosan-betamethasone dipropionate film group: chitosan sheets with betamethasone dipropionate were coated in nerve anastomosis. MNCV: Motor nerve conduction velocity; CMAP: compound muscle action potential; PDLLA: poly (D,L-lactic acid).

intensity was held at the lowest level (1 mA) according to the muscle reaction. The filter was set at 1 Hz–5 kHz, sweep speed was 1 ms/div, and sensitivity was 0.5 mV/div. Latency was calculated from the onset of CMAP, with conduction velocity of the fastest fiber given. Baseline to peak amplitude was also measured; this shows the numbers of fibers activated by nerve stimulation.

Statistical analysis

Each test was performed in triplicate. The results are shown as the mean ± SD. Differences between more than two groups were calculated by analysis of variance followed by Bonferroni *post hoc* test with SPSS 18.0 software (IBM, Armonk, NY, USA). GraphPad Prism 6.0 software (GraphPad Company, San Diego, CA, USA) was used for non-linear regression fitting analyses. A value of P less than 0.05 was considered statistically significant.

Results

Characteristics of chitosan sheets

We assumed that once the sheets became hydrated, the swelling medium would absorb betamethasone dipropionate. In this study, we used PBS as the hydrating medium. Swelling rate was calculated by weighing each sample before and after immersion at 37°C for 24 hours. After soaking in PBS, neutralized and dried chitosan sheets immediately swelled (within approximately one minute), which was constantly retained over time (**Figure 1**). Non-linear regression analysis showed that the constant rate was 2.073 ± 0.352 min^{-1} (half-time of approximately 0.36 minutes). Further, mechanical integrity of the films was retained in optimum condition until the test was finished. Nonetheless, sheets that were not subjected to the neutralization process dissolved quickly, as expected (data not shown). Films reached their maximum swelling after a few minutes. Hence, the delivery system was ready for drug release by a diffusion mechanism.

Drug release assay

To investigate drug release, we used several different experimental methods. First, we measured drug quantity released by diffusion as a function of contact time. We dissolved the sheet and measured the drug remaining at the end of the experiment (7 days of contact exposure). Bradford micro assay (**Figure 2**) showed that the drug was not detected before two consecutive days, and was released after five consecutive days. The drug quantity released over the time course was close to the detection limitation. Even after 7 days, almost 85% of the initial drug remained in the sheet. Furthermore, MTT assay showed that *in vitro* L929 cell viability was not significant in the control, PDLLA, and chitosan-betamethasone dipropionate film groups (**Figure 3**).

Dissolution of the carrier itself in the biological environ-

ment may be another possibility for drug delivery. We examined dissolution of chitosan sheets at different pH values, which ranged from acidic to normal physiological pH values (pH 3, 4, 5, 6, and 7.4). The results indicate that dissolution was faster at lower pH values, with the sheet totally dissolved at pH 3 after 10 hours, while it was unaffected when exposed to neutral pH values (**Figure 4**).

Chitosan-collagen betamethasone dipropionate film promotes nerve repair

Next, we examined the effect of chitosan-collagen betamethasone dipropionate films in repair of nerve injury. As described in the Materials and Methods, the tibial nerve was cut at the site 1 cm above the knee. Nerve stumps were sutured under microscopy and wounds treated with either chitosan-collagen betamethasone dipropionate film or PDLLA. We observed drug retention, scar formation, and nerve adhesion to scars at 4, 8, and 12 weeks after surgery. At 4 weeks after surgery, the shape of the chitosan-collagen betamethasone dipropionate film was normal, while it was significantly degraded with PDLLA (data not shown). At 8 weeks after surgery, the chitosan-collagen betamethasone dipropionate film was visibly degraded (data not shown). At 12 weeks after surgery, treatment with the chitosan-collagen betamethasone dipropionate film showed an improved effect on nerve repair compared with the control group (**Figure 5**). We found there was much less adhesion to the surrounding tissue in the chitosan-collagen betamethasone dipropionate film group. In all experimental groups, the incision healed well without secondary infection.

Histological assay for nerve regeneration

We performed immunocytochemical staining of nerve fibers for morphological observation. We found more nerve fibers with straighter growth in chitosan-collagen betamethasone dipropionate film-treated rats (**Figure 6**).

Electrophysiological study of nerve function

We determined whether nerve fiber function was improved in chitosan-collagen betamethasone dipropionate film-treated rats compared with the control group. Electrophysiological study showed that chitosan-collagen betamethasone dipropionate film treated-nerve fibers had improved function compared with the control group. At 8 weeks after surgery, CMAP was detected in all groups in response to stimulation of distal, proximal, or the conduit portion of nerve fibers. MNCV and CMAP amplitude in the control group were significantly lower compared with the PDLLA and chitosan-betamethasone dipropionate film groups ($P < 0.05$). However, there was no significant difference in MNCV or CMAP amplitude between PDLLA and chitosan-betamethasone dipropionate film groups ($P > 0.05$). At 12 weeks after surgery, there was no significant difference in MNCV between PDLLA and chitosan-betamethasone dipropionate film groups ($P > 0.05$), with a significant difference in CMAP amplitude ($P < 0.05$; **Figure 7**).

Discussion

Axons can regenerate successfully to restore functional connections in the peripheral nervous system (Benowitz et al., 2011; He et al., 2016; Hernandez-Morato et al., 2016). Formation of fibroblastic scars is a major problem in nerve repair, and inhibits regeneration of repaired nerves. Although scar formation is important for normal wound healing, scarring has side effects in many clinical situations (O'Kane et al., 1997). Scarring around a repaired peripheral nerve can significantly impede axonal sprouting and regeneration, which may lead to an unfavorable prognosis (Adams et al., 2016; Geuna et al., 2016; Levi et al., 2016).

Approximately half of regenerating axons may develop into scar tissue, even in well repaired nerve, which leads to local neuroma and impedes axonal regeneration to the target. Scarring is much worse in the event of any tension, which makes it almost impossible for axons to cross the nerve anastomosis and reach the distal part of the nerve. The reason why fibroblastic scar tissue is so uncompromising is unknown, especially as axons grow reasonably well on fibroblasts (Ozay et al., 2007; Albayrak et al., 2010; Park et al., 2011; Gocmen et al., 2012). Recently, studies have shown that endoneurial and perineurial fibroblasts (which are the main scar-forming cells) produce the proteoglycan, neural/glial antigen 2 (NG2), which is a considerable inhibitor of axonal regeneration (Hossain-lbrahim et al., 2007). The amount of glycosaminoglycan chain attached to NG2 increases dramatically in response to injury, which may lead to its inhibition. Further, there is a great increase in NG2 within scar domains blocking regeneration in injured human nerves (Fiorentino et al., 1991; Scherer et al., 1993; Kiefer et al., 1995; O'Keefe et al., 1999; Rezajooi et al., 2004; Bhatheja et al., 2006).

Chitosan is a natural aminopolysaccharide obtained by deacetylation of chitin that has been used as a drug-delivery vehicle because of its favorable biological properties including bioactivity, biocompatibility, positive charge, low immunogenicity, and biodegradability (Kumar et al., 2004; Cherukuri et al., 2017; Cho et al., 2017; Li et al., 2017). Various carriers that originate from chitosan have been developed as drug delivery systems. Chitosan- and anionic alginate-coated poly (d,l-lactide-co-glycolide) nanoparticles are suitable for delivery of bioactive resveratrol (Sanna et al., 2012). Encapsulation of resveratrol into optimized polymeric nanoparticles provides improved drug loading, effective controlled release, and protection against light-exposure degradation, thereby opening new perspectives for delivery of bioactivity-related phytochemicals for (nano) chemoprevention/chemotherapy (Sanna et al., 2012; Liu et al., 2017). Jayaraman et al. (2012) described the synthesis and use of an efficient nano-carrier molecule for retinal delivery of a nano-chitosan peptide, which was an excellent carrier for retinal drug delivery and had the potential to treat age-related macular degeneration. However, its clinical applications remain to be further investigated (Yu et al., 2012).

In our study, we developed a new method to delay scar formation. We used chitosan-collagen betamethasone dipro-

pionate film to ensure the drug remained longer in wounds, and allowed the nerve fiber to sprout and regenerate effectively and fix the injured neural network. To investigate sheet characteristics, several different experimental methods were used. The sheets reached their maximum swelling in two minutes, which suggests they enable drug release through a diffusion mechanism. Almost 85% of the initial drug was retained in the sheet, even after 7 days. Furthermore, the MTT test was performed to quantify cell viability, and showed that the sheets did not influence cell proliferation *in vitro*. In physiological environments, wound acidification is part of the process as the wound-healing process begins with hemostasis and inflammation. Accordingly, we examined chitosan sheet dissolution at different pH values, which showed that a faster dissolution process at lower pH values, while it was unaffected when soaked at neutral pH values. These findings show that the sheets have favorable biological properties, the most important point being that they performed significantly better than the control group during the experimental procedure *in vivo*. Additionally, chitosan-collagen is harmless, bioabsorbable, and suitable for surgery.

Our data demonstrate that chitosan-betamethasone dipropionate film is a promising material to improve functional nerve fiber regeneration in surgery.

Acknowledgments: *We are very grateful to Dr. Xu-yun Hua for valuable advice and support.*
Author contributions: *JJJ contributed to the conception and design of the study. PY and HYL wrote the paper and provided critical revision of the paper for intellectual content. PL contributed to statistical analysis and interpretation of data. All authors approved the final version of the paper.*
Conflicts of interest: *None declared.*
Financial support: *None.*
Research ethics: *The study protocol was approved by the Animal Ethics Committee of Hangzhou Plastic Surgery Hospital of China (approval number: LY12H05005). The experimental procedure followed the United States National Institutes of Health Guide for the Care and Use of Laboratory Animals (NIH Publication No. 85-23, revised 1985).*
Data sharing statement: *Datasets analyzed during the current study are available from the corresponding author on reasonable request.*
Plagiarism check: *Checked twice by iThenticate.*
Peer review: *Externally peer reviewed.*

References

Abarrategi A, Civantos A, Ramos V, Sanz Casado JV, Lopez-Lacomba JL (2008) Chitosan film as rhBMP2 carrier: delivery properties for bone tissue application. Biomacromolecules 9:711-718.

Adams RD, Willits RK, Harkins AB (2016) Computational modeling of neurons: intensity-duration relationship of extracellular electrical stimulation for changes in intracellular calcium. J Neurophysiol 115:602-616.

Albayrak BS, Ismailoglu O, Ilbay K, Yaka U, Tanriover G, Gorgulu A, Demir N (2010) Doxorubicin for prevention of epineurial fibrosis in a rat tibias nerve model: outcome based on gross postsurgical, histopathological, and ultrastructural findings. J Neurosurg Spine 12:327-333.

Arkoun M, Daigle F, Heuzey MC, Ajji A (2017) Mechanism of action of electrospun chitosan-based nanofibers against meat spoilage and pathogenic bacteria. Molecules 22:E585.

Barahuie F, Dorniani D, Saifullah B, Gothai S, Hussein MZ, Pandurangan AK, Arulselvan P, Norhaizan ME (2017) Sustained release of anticancer agent phytic acid from its chitosan-coated magnetic nanoparticles for drug-delivery system. Int J Nanomed 12:2361-2372.

Belkas JS, Shoichet MS, Midha R (2004) Peripheral nerve regeneration through guidance tubes. Neurol Res 26:151-160.

Benowitz LI, Popovich PG (2011) Inflammation and axon regeneration. Curr Opin Neurol 24:577-583.

Bhatheja K, Field J (2006) Schwann cells: origins and role in axonal maintenance and regeneration. Int J Biochem Cell Biol 38:1995-1999.

Cherukuri S, Batchu UR, Mandava K, Cherukuri V, Ganapuram KR (2017) Formulation and evaluation of transdermal drug delivery of topiramate. Int J Pharm Investig 7:10-17.

Cho SH, Kim A, Shin W, Heo MB, Noh HJ, Hong KS, Cho JH, Lim YT (2017) Photothermal-modulated drug delivery and magnetic relaxation based on collagen/poly(γ-glutamic acid) hydrogel. Int J Nanomed 12:2607-2620.

Eidlitz-Markus T, Kivity S, Goldberg-Stern H, Haimi-Cohen Y, Zeharia A (2012) Effect of high-dose glucocorticosteroid treatment for infantile spasms on quantitative bone parameters later in life. J Child Neurol 27:74-79.

Fiorentino DF, Zlotnik A, Mosmann TR, Howard M, O'Garra A (1991) IL-10 inhibits cytokine production by activated macrophages. J Immunol 147:3815-3822.

Ganguly S, Dash AK (2004) A novel in situ gel for sustained drug delivery and targeting. Int J Pharm 276:83-92.

Geuna S, Raimondo S, Fregnan F, Haastert-Talini K, Grothe C (2016) In vitro models for peripheral nerve regeneration. Eur J Neurosci 43:287-296.

Ghaznavi AM, Kokai LE, Lovett ML, Kaplan DL, Marra KG (2011) Silk fibroin conduits: a cellular and functional assessment of peripheral nerve repair. Ann Plast Surg 66:273-279.

Gocmen S, Sirin S, Oysul K, Ulas UH, Oztas E (2012) The effects of low-dose radiation in the treatment of tibias nerve injury in rats. Turk Neurosurg 22:167-173.

Grauer O, Offenhausser M, Schmidt J, Toyka KV, Gold R (2001) Glucocorticosteroid therapy in optic neuritis and multiple sclerosis: evidence from clinical studies and practical recommendations Nervenarzt 72:577-589.

He X, Ao Q, Wei Y, Song J (2016) Transplantation of miRNA-34a overexpressing adipose-derived stem cell enhances rat nerve regeneration. Wound Repair Regen 24:542-550.

Hernandez-Morato I, Sharma S, Pitman MJ (2016) Changes in neurotrophic factors of adult rat laryngeal muscles during nerve regeneration. Neuroscience 333:44-53.

Heux L, Brugnerotto J, DesbrieresJ, Versali MF, Rinaudo M (2000) Solid state NMR for determination of degree of acetylation of chitin and chitosan. Biomacromolecules 1:746-751.

Hossain-Ibrahim MK, Rezajooi K, Stallcup WB, Lieberman AR, Anderson PN (2007) Analysis of axonal regeneration in the central and peripheral nervous systems of the NG2-deficient mouse. BMC Neurosci 8:80.

Hsu SH, Su CH, Chiu IM (2009) A novel approach to align adult neural stem cells on micropatterned conduits for peripheral nerve regeneration: a feasibility study. Artif Organs 33:26-35.

Isaacs JE, Cheatham S, Gagnon EB, Razavi A, McDowell CL (2008) Reverse end-to-side neurotization in a regenerating nerve. J Reconstr Microsurg 24:489-496.

Janes KA, Fresneau MP, Marazuela A, Fabra A, Alonso MJ (2001) Chitosan nanoparticles as delivery systems for doxorubicin. J Control Release 73:255-267.

Jayakumar R, New N, Tokura S, Tamura H (2007) Sulfated chitin and chitosan as novel biomaterials. Int J Biol Macromol 40:175-181.

Jayaraman MS, Bharali DJ, Sudha T, Mousa SA (2012) Nano chitosan peptide as a potential therapeutic carrier for retinal delivery to treat age-related macular degeneration. Mol Vis 18:2300-2308.

Joseph MS, Bilousova T, Zdunowski S, Wu ZP, Middleton B, Boudzinskaia M, Wong B, Ali N, Zhong H, Yong J, Washburn L, Escande-Beillard N, Dang H, Edgerton VR, Tillakaratne NJ, KaufmanDL (2011) Transgenic mice with enhanced neuronal major histocompatibility complex class I expression recover locomotor function better after spinal cord injury. J Neurosci Res 89:365-372.

Kiefer R, Streit WJ, Toyka KV, Kreutzberg GW, Hartung HP (1995) Transforming growth factor-beta 1: a lesion-associated cytokine of the nervous system. Int J Dev Neurosci 13:331-339.

Kim ES, Frampton JE (2017) Calcipotriol/betamethasone dipropionate foam: a review in plaque psoriasis. Drugs 76:1485-1492.

Kumar MN, Muzzarelli RA, Muzzarelli C, Sashiwa H, Domb AJ (2004) Chitosan chemistry and pharmaceutical perspectives. Chem Rev 104:6017-6084.

Levi AD, Burks SS, Anderson KD, Dididze M, Khan A, Dietrich WD (2016) The use of autologous Schwann cells to supplement tibias nerve repair with a large gap: first in human experience. Cell Transplant 25:1395-1403.

Li J, Deng J, Yuan J, Fu J, Li X, Tong A, Wang Y, Chen Y, Guo G (2017) Zonisamide-loaded triblock copolymer nanomicelles as a novel drug delivery system for the treatment of acute spinal cord injury. Int J Nanomed 12:2443-2456.

Liang H, Sheng F, Zhou B, Pei Y, Li B, Li J (2017) Phosphoprotein/chitosan electrospun nanofibrous scaffold for biomineralization. Int J Biol Macromol 102:218-224.

Liu C, Liu XN, Wang GL, Hei Y, Meng S, Yang LF, Yuan L, Xie Y (2017) A dual-mediated liposomal drug delivery system targeting the brain: rational construction, integrity evaluation across the blood-brain barrier, and the transporting mechanism to glioma cells. Int J Nanomed 12:2407-2425.

Lovato P, Norsgaard H, Tokura Y, Røpke MA (2016) Corrigendum to "Calcipotriol and betamethasone dipropionate exert additive inhibitory effects on the cytokine expression of inflammatory dendritic cell-Th17 cell axis in psoriasis". J Dermatol Sci 81:153-164.

Mandracchia D, Trapani A, Tripodo G, Perrone MG, Giammona G, Trapani G, Colabufo NA (2017) In vitro evaluation of glycol chitosan based formulations as oral delivery systems for efflux pump inhibition. Carbohydr Polym 166:73-82.

Mi FL, Shyu SS, Wu YB, Lee ST, Shyong JY, Huang RN (2001) Fabrication and characterization of a sponge-like asymmetric chitosan membrane as a wound dressing. Biomaterials 22:165-173.

Mi FL, Wu YB, Shyu SS, Schoung JY, Huang YB, Tsai YH, Hao JY (2002) Control of wound infections using a bilayer chitosan wound dressing with sustainable antibiotic delivery. J Biomed Mater Res 59:438-449.

Mitra S, Gaur U, Ghosh PC, Maitra AN (2001) Tumour targeted delivery of encapsulated dextran-doxorubicin conjugate using chitosan nanoparticles as carrier. J Control Release 74:317-323.

Ngeow WC (2010) Scar less: a review of methods of scar reduction at sites of peripheral nerve repair. Oral Surg Oral Med Oral Pathol Oral Radiol Endod 109:357-366.

Okamoto Y, Watanabe M, Miyatake K, Morimoto M, Shigemasa Y, Minami S (2002) Effects of chitin/chitosan and their oligomers/monomers on migrations of fibroblasts and vascular endothelium. Biomaterials 23:1975-1979.

O'Kane S, Ferguson MW (1997) Transforming growth factor beta s and wound healing. Int J Biochem Cell Biol 29:63-78.

O'Keefe GM, Nguyen VT, Benveniste EN (1999) Class II transactivator and class II MHC gene expression in microglia: modulation by the cytokines TGF-beta, IL-4, IL-13 and IL-10. Eur J Immunol 29:1275-1285.

Ozay R, Bekar A, Kocaeli H, Karli N, Filiz G, Ulus IH (2007) Citicoline improves functional recovery, promotes nerve regeneration, and reduces postoperative scarring after peripheral nerve surgery in rats. Surg Neurol 68:615-622.

Park JS, Lee JH, Han CS, Chung DW, Kim GY (2011) Effect of hyaluronic acid-carboxymethylcellulose solution on perineural scar formation after tibias nerve repair in rats. Clin Orthop Surg 3:315-324.

Paul C, Bang B, Lebwohl M (2017) Fixed combination calcipotriol plus betamethasone dipropionate aerosol foam in the treatment of psoriasis vulgaris: rationale for development and clinical profile. Expert Opin Pharmacother 18:115-121.

Praphakar RA, Munusamy MA, Rajan M (2017) Development of extended-voyaging anti-oxidant linked amphiphilic polymeric nanomicelles for anti-tuberculosis drug delivery. Int J Pharm 524:168-177.

Qiu S, Wang J (2017) The prediction of food additives in the fruit juice based on electronic nose with chemometrics. Food Chem 230:208-214.

Queille-Roussel C, Bang B, Clonier F, Lacour JP (2016) Enhanced vasoconstrictor potency of the fixed combination calcipotriol plus betamethasone dipropionate in an innovative aerosol foam formulation vs. other corticosteroid psoriasis treatments. J Eur Acad Dermatol Venereol 30:1951-1956.

Rezajooi K, Pavlides M, Winterbottom J, Stallcup WB, Hamlyn PJ, LiebermanAR, Anderson PN (2004) NG2 proteoglycan expression in the peripheral nervous system: upregulation following injury and comparison with CNS lesions. Mol Cell Neurosci 25:572-584.

Sall KN, Kreter JK, Keates RH (1987) The effect of chitosan on corneal wound healing. Ann Ophthalmol 19:31-33.

Sanna V, Roggio AM, Siliani S, Piccinini M, Marceddu S, Mariani A, Sechi M (2012) Development of novel cationic chitosan-and anionic alginate-coated poly (D,L-lactide-co-glycolide) nanoparticles for controlled release and light protection of resveratrol. Int J Nanomed 7:5501-5516.

Scherer SS, Kamholz J, Jakowlew SB (1993) Axons modulate the expression of transforming growth factor-betas in Schwann cells. Glia 8:265-276.

Sedy J (2010) Traumatic neuroma and scar tissue. Int J Oral Maxillofac Surg 39:310-311.

Takezawa T, Takeuchi T, Nitani A, Takayama Y, Kino-Oka M, Taya M, Enosawa S (2007) Collagen vitrigel membrane useful for paracrine assays in vitro and drug delivery systems in vivo. J Biotechnol 131:76-83.

Vanden Braber NL, Díaz Vergara LI, Morán Vieyra FE, Borsarelli CD, Yossen MM, Vega JR, Correa SG, Montenegro MA (2017) Physicochemical characterization of water-soluble chitosan derivatives with singlet oxygen quenching and antibacterial capabilities. Int J Biol Macromol 102:200-207.

Xiao Y, Ge H, Zou S, Wen H, Li Y, Fan L, Xiao L (2017) Enzymatic synthesis of N-succinyl chitosan-collagen peptide copolymer and its characterization. Carbohydr Polym 166:45-54.

Yin Y, Dang Q, Liu C, Yan J, Cha D, Yu Z, Cao Y, Wang Y, Fan B (2017) Itaconic acid grafted carboxymethyl chitosan and its nanoparticles: preparation, characterization and evaluation. Int J Biol Macromol 102:10-18.

Yohn DC, Miles GB, Rafuse VF, Brownstone RM (2008) Transplanted mouse embryonic stem-cell-derived motoneurons form functional motor units and reduce muscle atrophy. J Neurosci 28:12409-12418.

Yu J, Xie X, Zheng M, Yu L, Zhang L, Zhao J, Jiang D, Che X (2012) Fabrication and characterization of nuclear localization signal-conjugated glycol chitosan micelles for improving the nuclear delivery of doxorubicin. Int J Nanomed 7:5079-5090.

Zheng Y, Su C, Zhao L, Shi Y (2017) Chitosan nanoparticle-mediated co-delivery of shAtg-5 and gefitinib synergistically promoted the efficacy of chemotherapeutics through the modulation of autophagy. J Nanobiotechnol 5:28.

(*Copyedited by James R, Raye W, Wang J, Li CH, Qiu Y, Song LP, Zhao M*)